

Superconducting microwave cavity towards controlling the motion of polar molecules

Katsunari Enomoto · Pavle Djuricanin · Ilja Gerhardt · Omid Nourbakhsh · Yoshiki Moriwaki · Walter Hardy · Takamasa Momose

Received: 1 May 2012/Revised: 20 July 2012/Published online: 17 September 2012
© Springer-Verlag 2012

Abstract We propose the use of superconducting microwave cavities for the focusing and deceleration of cold polar molecular beams. A superconducting cavity with a high quality factor produces a large ac Stark shift in polar molecules, which allow us to efficiently control molecular motion. Our discussion is based on the experimental characterization of a prototype cavity: a lead–tin-coated cylindrical copper cavity, which has a quality factor of 10^6 and tolerates several watts of input power. Such a microwave device provides a powerful way to control molecules not only in low-field-seeking states, but also in high-field-seeking states such as the ground rotational state.

1 Introduction

Control of the translational motion of molecular beams has been a challenge in molecular physics and spectroscopy for a long time since the historical Stern–Gerlach experiment [1–3]. Recently, various methods have been rapidly

developed aiming for the generation of trapped ultracold molecular gases. Helium buffer-gas cooling combined with a superconducting magnetic trap allows one to confine paramagnetic molecular gases at sub-Kelvin temperatures [4]. So-called Stark decelerators decelerate polar molecules and load them into various kinds of traps [5, 6]. Stark velocity filters with bent multipole electrodes extract slow molecules from an ensemble at high temperatures [7, 8]. Zeeman decelerators for paramagnetic atoms and molecules have also been realized [9, 10]. These techniques have been applied for studies on cold collisions of molecules in well-defined internal states with atoms, molecules, and ions [11, 12]. Cold molecules are also of great interest for precision measurements of fundamental quantities in particle physics. For example, the newest upper limit on the magnitude of the permanent electric dipole moment of the electron is given by a molecular-beam-based experiment [13].

Most of the devices to confine molecules in free space use static electric or magnetic fields, which is, in principle, only applicable to low-field-seeking (LFS) states as provided by Earnshaw's theorem. However, high-field seeking (HFS) states are practically of more interest, as the lowest-energy rotational state of molecules is the HFS state for static fields. In addition, low-lying rotational states with small rotational constants become HFS states at strong static electric fields. Dynamical confinement using quasi-static fields is one of the methods to control HFS states. Guides [14, 15], decelerators [16–18], and traps [6] for HFS state molecules using this technique have been demonstrated, but the effective confinement potential of these methods is typically tens of milli-Kelvins. Note that a static field guide using a thin wire was also realized [19, 20]. Another method to control HFS states is the use of the dipole force generated by high-intensity electromagnetic

K. Enomoto (✉) · Y. Moriwaki
Department of Physics, University of Toyama,
3190 Gofuku, Toyama, 930-8555, Japan
e-mail: enomoto@sci.u-toyama.ac.jp

P. Djuricanin · I. Gerhardt · T. Momose
Department of Chemistry, The University of British Columbia,
Vancouver BC V6T 1Z1, Canada
e-mail: momose@chem.ubc.ca

O. Nourbakhsh · W. Hardy · T. Momose
Department of Physics and Astronomy,
The University of British Columbia,
Vancouver BC V6T 1Z1, Canada

waves. Cooling and deceleration methods with near- and mid-infrared optical fields have also been proposed and demonstrated [21–26]. DeMille and co-workers have proposed a trap for polar molecules using standing waves of microwave fields enhanced in a cavity [27, 28]. In terms of the size and depth of the trapping potential, the use of standing microwave fields in a cavity has advantages over shorter wavelength optical fields. The microwave trap may reach a trap depth up to a few Kelvin with a size on the order of the microwave wavelength. We have proposed a deceleration method for polar molecules in HFS states using time-varying microwave standing waves [29]. As early as 1975, a molecular beam deflector using resonant microwave fields was demonstrated for CsF molecules [30]. Very recently, molecular beam focusing [31] and deceleration [32] were achieved, in which a slow ammonia beam of well-defined velocity and internal states was used. Collision mechanisms in microwave traps have also been investigated theoretically [33, 34].

In this paper, we discuss the control of translational motion of molecules in a superconducting microwave cavity. The recent experiments of the molecular beam focusing [31] and deceleration [32] by the dipole force of near-resonant microwave radiation used normal-conductor copper cavities with a quality factor of about 10^4 . The degree of deceleration and focusing is much improved by adopting a superconducting cavity because of its much higher quality factor. As the superconductor cavity requires a cryogenic environment, it may be natural to combine it with cold molecular beam sources based on helium buffer-gas cooling in the future [35]. So far, state-of-the-art superconducting cavities have quality factors of about 10^{10} , which have been used for charged particle accelerators [36] and cavity quantum electrodynamics experiments [37, 38]. As we discuss in this paper, a high quality factor on the order of 10^{10} is not required or even not favored for the purpose of constructing a microwave molecular decelerator, as it requires fast switching of the microwaves, which is not possible with a very high quality factor. Here, we discuss a prototype cylindrical superconducting cavity with a moderately high quality factor of about 10^6 . The cavity was characterized by applying microwaves of several watts on a sub-second time scale. Based on the observed performance of the cavity and theoretical simulations, we quantitatively discuss the efficiency of the deceleration and focusing of molecules. Section 2 summarizes theories relevant to the microwave cavity and control of translational motion of molecules. Experimental procedures and results for the characterization of the cavity are described in Sect. 3. The efficiency of the deceleration and focusing is discussed in Sect. 4.

2 Principle and theory

Here, we describe the basics for the control of translational motion of polar molecules by the use of the ac Stark shift of near resonant microwave fields in a cylindrical cavity. We consider two rotational states, $|e\rangle$ and $|g\rangle$, with the energy of E_e and E_g , respectively ($E_e > E_g$). The ac Stark shift U of the ground rotational state ($|g\rangle$) calculated under the rotating wave approximation and two-level approximation is given by

$$U = \frac{h(\nu_{\text{eg}} - \nu)}{2} \pm \sqrt{\left[\frac{h(\nu_{\text{eg}} - \nu)}{2}\right]^2 + \left(\frac{E\mu_{\text{eg}}}{2}\right)^2}, \quad (1)$$

where E is the electric field amplitude, h is the Planck constant, ν is the frequency of the microwave, $\nu_{\text{eg}} = (E_e - E_g)/h$ is the transition frequency, and μ_{eg} is the transition dipole moment between the two states. The sign in (1) depends on the sign of the detuning $\nu_{\text{eg}} - \nu$; the + sign is for $\nu > \nu_{\text{eg}}$, and the – sign is for $\nu < \nu_{\text{eg}}$. For near-resonant and high-power microwaves, namely $h|\nu_{\text{eg}} - \nu| \ll E\mu_{\text{eg}}$, the ac Stark shift is linear in the electric field and insensitive to the detuning $|\nu_{\text{eg}} - \nu|$. More rigorous calculation for the ac Stark shift can be done by the dressed-state formalism [27]. Figure 1 shows the ac Stark shift of the ground state of acetonitrile (CH_3CN). The $J = 1$ and $J = 0$ states correspond to the $|e\rangle$ and $|g\rangle$ states, respectively. Here, we ignore the hyperfine structure. The dressed state formalism predicts an avoided crossing due to a

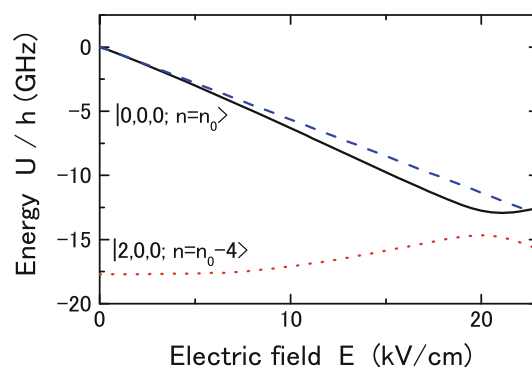


Fig. 1 Ac Stark shift of the acetonitrile molecule in the ground rotational state ($J = 0$) calculated by (1) (dashed line) and the dressed-state treatment (solid line). The parameters used are $\nu_{\text{eg}} = 18.4$ GHz and $\nu = 18.3$ GHz. The dipole moment of CH_3CN is 3.92 debye [39], and the transition dipole moment between $|J, K, M = 0, 0, 0\rangle$ and $|1, 0, 0\rangle$ states is $\mu_{\text{eg}} = \langle 1, 0, 0 | \mu | 0, 0, 0 \rangle = 3.92/\sqrt{3} = 2.26$ debye, where J is the rotational quantum number, and K and M refer to the rotational angular-momentum projections on the molecule-fixed and space-fixed axes, respectively. There is an avoided crossing between the $|J, K, M; n\rangle = |0, 0, 0; n_0\rangle$ ground state and the $|2, 0, 0; n_0 - 4\rangle$ state (dotted line), where n is the dressed-state photon number

Table 1 Basic formulae for the TE_{11p}, TE_{01p}, and TM_{01p} modes of a cylindrical cavity [40, 41]

	TE _{11p} mode ($p \geq 1$)	TE _{01p} mode ($p \geq 1$)	TM _{01p} mode ($p \geq 0$)
v_p	$\frac{c}{2a} \sqrt{\left(\frac{x'_{11}}{\pi}\right)^2 + \left(\frac{pa}{d}\right)^2}$	$\frac{c}{2a} \sqrt{\left(\frac{x'_{01}}{\pi}\right)^2 + \left(\frac{pa}{d}\right)^2}$	$\frac{c}{2a} \sqrt{\left(\frac{x_{01}}{\pi}\right)^2 + \left(\frac{pa}{d}\right)^2}$
E_ρ	$E_0 \frac{J_1(x'_{11}\rho/a)}{x'_{11}\rho/a} \sin \theta \sin \frac{\pi pz}{d}$	0	$-E_0 \frac{\pi pa}{x_{01}d} J'_0(x_{01}\rho/a) \sin \frac{\pi pz}{d}$
E_θ	$E_0 J'_1(x'_{11}\rho/a) \cos \theta \sin \frac{\pi pz}{d}$	$E_0 J'_0(x'_{01}\rho/a) \sin \frac{\pi pz}{d}$	0
E_z	0	0	$E_0 J_0(x_{01}\rho/a) \cos \frac{\pi pz}{d}$
W	$\frac{\epsilon_0 E_0^2 \pi a^2 d}{8} \left(1 - \frac{1}{x_{11}^2}\right) J_1^2(x'_{11})$ $\simeq 0.02984 \epsilon_0 E_0^2 V$	$\frac{\epsilon_0 E_0^2 \pi a^2 d}{4} J_0^2(x'_{01})$ $\simeq 0.04055 \epsilon_0 E_0^2 V$	$\frac{\epsilon_0 E_0^2 \pi a^2 d}{2s_p} \left[1 + \left(\frac{\pi pa}{x_{01}d}\right)^2\right] J_1^2(x_{01})$ $\simeq 0.1348 \epsilon_0 E_0^2 V$ ($p = 0$)
Q_r	$\frac{c\mu_0}{2R_s} \frac{(x'_{11})^2 - 1 [x'_{11})^2 + (\pi pa/d)^2]^{\frac{3}{2}}}{x'_{11}{}^4 + 2\pi^2 p^2 x'_{11}{}^2 a^3/d^3 + (\pi pa/d)^2 (1 - 2a/d)}$	$\frac{c\mu_0}{2R_s} \frac{[x'_{01})^2 + (\pi pa/d)^2]^{\frac{3}{2}}}{x'_{01}{}^4 + 2\pi^2 p^2 a^3/d^3}$	$\frac{c\mu_0}{2R_s} \frac{\sqrt{x_{01}^2 + (\pi pa/d)^2}}{1 + s_p a/d}$

Resonant frequencies, v_p , electric field component amplitudes, E_ρ, E_θ, E_z , the total energy, W , stored in the cavity, and the quality factor due to the surface resistance, Q_r , for a closed cavity are listed, where $\{\rho, \theta, z\}$ are radial, azimuthal, and axial components, respectively, of the cylindrical coordinate system whose origin is at the center of one of the ends of the cavity. J_m and J'_m refer respectively to the m -th order Bessel function and its derivative. x_{mn} and x'_{mn} are respectively n -th roots of J_m and J'_m , that is, $x'_{11} = 1.8412$, $x'_{01} = 3.8317$, and $x_{01} = 2.4048$. a and d are the radius and the length of the cavity, respectively, and $V = \pi a^2 d$ is the volume. ϵ_0 and μ_0 are permittivity and permeability of vacuum, respectively. c is the speed of light in vacuum. $s_p = 1$ for $p = 0$ and $s_p = 2$ for $p \neq 0$. Note that the maximum electric field amplitude is $E_0/2$ for the TE_{11p} mode, $0.582E_0$ for the TE_{01p} mode, and E_0 for the TM₀₁₀ mode

multiphoton transition. The magnitude of the electric field discussed in this paper is in the range where this level crossing does not occur, and therefore, the rest of the discussion is based on the ac Stark shift given by (1).

The principle of the microwave decelerator is similar to that of the static Stark decelerator [5]. The space-varying amplitude of the electric field of the microwave provides a force on the molecules, and time-varying amplitude of the electric field changes the kinetic energy of the molecules, resulting in deceleration (or acceleration). The molecules traveling along the axis of the cavity experience a series of hills and troughs of ac Stark shift potentials due to the standing waves. If the standing wave is repeatedly turned on and off in accordance with the timing of the flight of a specific molecule, called a synchronous molecule, a molecular packet around the synchronous molecule in phase space will be decelerated. The efficiency of the deceleration is much improved using a cylindrical cavity, instead of a Fabry–Perot cavity as in our original proposal [29].

Here, the microwave frequency range of interest is 1–100 GHz, which covers the rotational transitions of most simple molecules, Λ -doublet transitions of Π electronic states, as well as low frequency vibrational transitions such as the inversion transition of ammonia. This frequency range makes the size of cavity compatible with the size of standard molecular beams. The cavity has a circular hole at the center of each end to introduce a molecular beam into the cavity. The size of the hole is much less than the microwave wavelength in order to maintain a high quality factor of the cavity.

An advantage of using a microwave field is that a field maximum is obtained in free space, which is impossible for a dc electric field (Earnshaw’s theorem). For example, the TM₀₁₀ mode has the maximum ac field amplitude on the longitudinal cavity axis (see Table 1 for the details of the electric field distribution). This field distribution provides a two-dimensional radial confinement harmonic potential for HFS states. Since the TM₀₁₀ mode does not have a node along the longitudinal cavity axis and the field pattern is axially symmetric, this mode is ideal for focusing HFS states. Another useful mode of a cylindrical cavity is the TE_{01p} mode where p is the number of longitudinal modes. This mode has zero ac electric field amplitude along the longitudinal cavity axis, which provides two-dimensional radial confinement potential for LFS states.

The TE_{11p} mode has the lowest cutoff frequency among cylindrical cavity modes. This mode has maximum ac field amplitude on the center axis, which radially confines molecules in the HFS states. The field amplitude along the cavity axis changes periodically from zero to the maximum. As a result, the TE_{11p} mode provides a three-dimensional trapping potential for HFS states at every antinode. This periodic potential also allows deceleration of molecules traveling along the axis by switching the field. The radial confinement is an important advantage of the microwave decelerator as it conserves phase-space density of decelerated packets. Note that the radial confinement potential of the microwave decelerator is “static”. Another method for the deceleration of HFS states is the alternate gradient focusing decelerator [16], which uses a dynamically alternating potential for the radial confinement of

molecules. In terms of the stability of the phase space density, the “static” confinement potential of the microwave decelerator is advantageous compared to the “dynamic” confinement potential, especially near zero velocity.

Below, we discuss the quality factor of a cylindrical microwave cavity in more detail. The electric field pattern for each mode and the total energy W stored in the cavity are summarized in Table 1. The quality factor of the cavity is, in general, defined as $Q = 2\pi\nu W/P$, where P is the power loss of the cavity. The unloaded quality factor Q_0 of the cavity may be expressed as

$$\frac{1}{Q_0} = \frac{1}{Q_r} + \frac{1}{Q_d} + \frac{1}{Q_{\text{others}}}, \tag{2}$$

where Q_r , Q_d , and Q_{others} represent quality factors corresponding to power loss due to a finite surface resistance, loss due to the end holes, and other effects such as the coupling to a monitoring antenna and contact resistance among cavity parts, respectively. Each quality factor Q_i ($i = r, d, \text{others}$) is defined as $Q_i = 2\pi\nu W/P_i$, where P_i is the power loss due to each effect. The factor Q_r due to a finite surface resistance R_s is theoretically derived by the equation listed in Table 1. Based on the Bardeen–Cooper–Schrieffer theory, the temperature T and frequency ν dependences of R_s are approximated by [36]

$$R_s = R_{\text{res}} + R_{\text{BCS}}, R_{\text{BCS}} \propto \frac{\nu^b}{T} \exp\left(-\frac{\Delta}{k_B T}\right), \tag{3}$$

where R_{res} is the residual surface resistance at zero temperature, b is a frequency dependence factor, k_B is the Boltzmann constant, and 2Δ is the energy gap. The second term, R_{BCS} , represents the temperature dependence in R_s . Here we ignore the temperature dependence of Δ , which is valid for $h\nu \ll \Delta$ and $T \ll T_c$, where T_c is the critical temperature. In the case of lead ($T_c = 7.2$ K), Halbritter [42] reported the values of $\Delta/k_B = 15$ K, $b = 1.75$ for $\nu < 10$ GHz, and $R_{\text{BCS}} \simeq 11 \mu\Omega$ at 5 GHz and 4.17 K. If we simply extrapolate these values to $\nu = 18$ GHz, we obtain the surface resistance of lead at 18 GHz to be $R_{\text{BCS}} = 0.10$ m Ω at 4.17 K, and $R_{\text{BCS}} = 23 \mu\Omega$ at 2.7 K. The first term, R_{res} , depends on the surface condition, and is typically on the order of 0.1 $\mu\Omega$ if the surface is clean.

The two holes at both ends of the cylinder cause diffraction loss P_d . We consider a cylindrical hole of radius a_h and length d_h . It is known that the diffraction loss is proportional to a_h^6 if a_h is significantly smaller than the wavelength [43, 44]. By extending the length of the hole d_h , the loss decreases exponentially as the evanescent mode in the hole attenuates [40, 45]. Therefore, longer hole length, d_h , and smaller radius, a_h , are better in order to minimize the loss of the quality factor due to the holes.

However, shorter length, d_h , and larger radius, a_h , are better for the microwave cavity decelerator in order to increase the transmission of molecular beams through the cavity. For small a_h and long d_h , the power loss for each hole for the TE_{11p} mode is approximated by [40]

$$P_h = \frac{32\epsilon_0\pi^3\nu^4}{27c^3} a_h^6 E_0^2 \left[1 - \left(\frac{cx'_{11}}{2\pi\nu a} \right)^2 \right] e^{-2\gamma_m d_h}, \tag{4}$$

where $\gamma_m = \sqrt{(x'_{11}/a_h)^2 - (2\pi\nu/c)^2}$. For the TM_{01p} mode it is given by

$$P_h = \frac{32\epsilon_0\pi^3\nu^4}{27c^3} a_h^6 E_0^2 e^{-2\gamma_e d_h}, \tag{5}$$

where $\gamma_e = \sqrt{(x_{01}/a_h)^2 - (2\pi\nu/c)^2}$. The diffraction loss P_d is the sum of this power loss P_h due to each hole. For our prototype cavity, whose hole radius a_h is small and length d_h is long as will be described in Sect. 3, this diffraction loss is negligibly small. The relevant quality factor Q_d is higher than 10^{10} for both TE_{11p} and TM_{010} modes at about $\nu = 18$ GHz. Note that more rigorous analysis of such diffraction problems for a sub-wavelength and finite-thickness aperture can be discussed by considering the modal matching at the entrance and the exit of the aperture [46, 47].

The microwaves are fed through an antenna into the cavity. The quality factor of the total system including this input coupler is the observable. This quality factor is called the loaded quality factor, Q_L , which is related to the unloaded quality factor, Q_0 , as $Q_L^{-1} = Q_0^{-1} + Q_c^{-1}$, where Q_c is the quality factor due to the input coupler. The ratio $\beta = Q_0/Q_c$ is called the coupling parameter. Note that

$$Q_L = \frac{Q_0}{1 + \beta}. \tag{6}$$

When the microwave frequency is swept near a resonance and the reflected power is measured, the full width at half maximum $\delta\nu$ of the resonant signal in the frequency domain is related to Q_L as

$$Q_L = \frac{\nu_p}{\delta\nu}, \tag{7}$$

where ν_p is the resonant frequency. The loaded quality factor Q_L is also obtained from the time domain measurement. The decay of the stored energy $W(t)$ as a function of time t after sudden turning off of the microwave input is given by

$$W(t) = W(0)e^{-2\pi\nu t/Q_L}. \tag{8}$$

In the steady state and at resonance, the energy W is related to the unloaded quality factor Q_0 of the cavity and the input power P_{in} as

$$2\pi\nu W = P_{\text{in}}Q_0(1 - |\Gamma|^2) \\ = P_{\text{in}}Q_L \frac{4\beta}{1 + \beta}, \quad (9)$$

where Γ is the voltage reflection coefficient of the coupling antenna. Here, the voltage reflection coefficient, Γ , is related to the coupling parameter, β , as

$$|\Gamma|^2 = \left(\frac{1 - \beta}{1 + \beta}\right)^2. \quad (10)$$

At critical coupling, all the microwave power goes into the cavity and there is no reflection ($\Gamma = 0$), $\beta = 1$ and $Q_L = Q_0/2$.

3 Experiment and result

We have constructed a prototype superconducting cavity, and examined its ability to retain a high quality factor at high microwave powers of several watts. The cavity was made from copper and the inner surface was electrochemically plated with an alloy of lead and tin, which has a critical temperature $T_c = 7 - 8$ K [48]. The nominal cavity dimensions were: inner length $d = 162.8$ mm and inner radius $a = 6.35$ mm. The cavity was composed of a main body and two end caps. The main body included most of the cavity volume. Two circular holes of 2.3 mm diameter were located at the middle of the side wall of the main body to accept an input coupler antenna and monitoring antenna. The end caps had a centered hole for the entrance and exit of molecular beams. The radius of the entrance

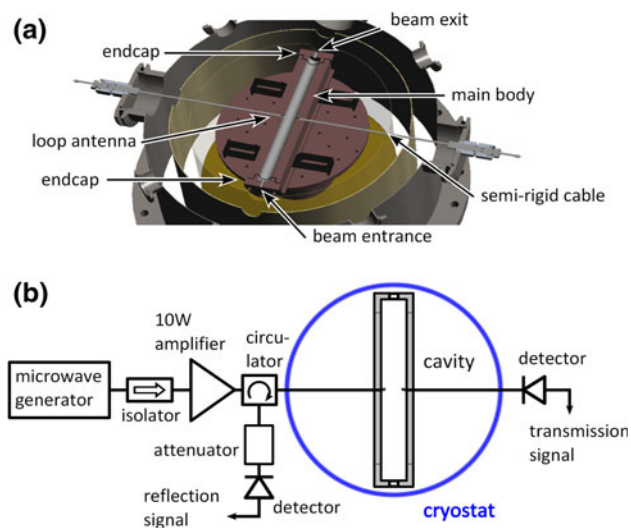


Fig. 2 Experimental setup for the characterization of the superconducting cavity. **a** Bottom view of the cavity and the cryostat. The cross section along the cavity axis is shown. **b** Block diagram for the measurements of reflection and transmission signals

hole was $a_h = 1.0$ mm and the exit hole was $a_h = 1.5$ mm. The length of the hole was $d_h = 6$ mm for both ends. The seam between the end cap and main body was located at 6.6 mm from each end of the cavity. The location of the seam was chosen such that the longitudinal surface current of the TE_{11p} mode at about 18.4 GHz ($p = 13$) was almost minimum at the seam line. Corners of the inner surface were slightly rounded to allow for efficient electroplating. The cavity was thermally attached to the bottom of a liquid helium bath cryostat via a copper block and indium sheets.

The two antennas inserted through the side holes were custom made loop antennas (diameter ≈ 1.5 mm) to magnetically couple the standing wave into the cavity. The loop was at the tip of a semi-rigid coaxial cable (Coax, SC-219/50-SCN-CN). The cable had a diameter of 2.2 mm, and its conductive material was silver-plated cupro-nickel, which has low thermal conductivity and low transmission loss. These cables were thermally anchored to the helium bath. To allow for the adjustment of the coupling strength, the feedthrough of these cables had a mechanical translational stage so that the position of the loop antennas could be controlled from outside the cryostat. The monitoring antenna was very weakly coupled to the cavity in order to maintain a high quality factor.

The experimental setup for the characterization of the cavity is illustrated in Fig. 2. Microwaves of about 18 GHz were generated by a microwave signal generator (Anritsu, MG3693C), and amplified by a solid-state power amplifier (Cernex, CNP18183040-01) to 10 W. After passing through a circulator, the microwaves were fed into the cavity via the semi-rigid cable and loop antenna. Due to the loss in the semi-rigid cable, about $P_{\text{in}} = 5$ W power was delivered to the cavity. Also, the reflected power from the cavity to the circulator was about 2 W at non-resonant frequency, due to the same loss. The reflection to the

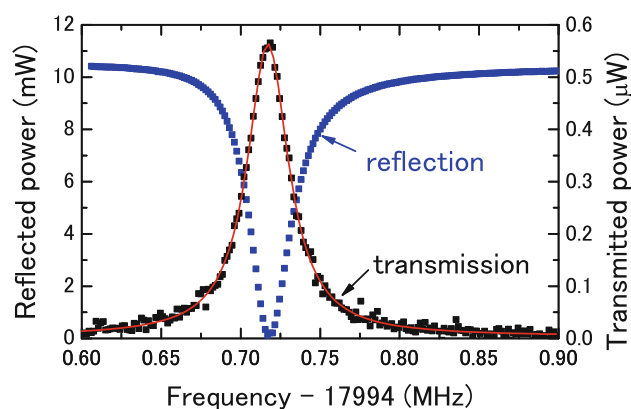


Fig. 3 Transmission and reflection signals of the superconducting cavity at the critical coupling. The resonant mode was TM_{010} . Dots are the experimental data and the red line shows a Lorentzian fit for the transmission signal

circulator was attenuated and then monitored with a diode detector (Agilent, 8473C). The same model detector was also connected to the cable of the monitoring antenna, and this transmission signal was amplified by a dc amplifier. The position of the input coupler antenna was optimized by minimizing the reflected power from the cavity at resonance. The reduction of the reflection was simultaneously monitored by the increase of the transmission signal. For experiments with high input power, pulsed microwaves were applied with the duration between 1 and 100 ms in order to reduce the thermal load to the cavity. By pumping the liquid helium, the cavity temperature was kept to 2.7 K. The temperature was monitored with a sensor attached outside of the cavity. The temperature of the cavity increased by about 0.2 K when a 5 W, 100 ms pulse was applied.

The loaded quality factor Q_L was measured via two methods; the resonance linewidth measurement of a microwave frequency scan and the transient signal measurement for a microwave pulse. For the measurement of the resonance linewidth, we applied cw microwaves of 0.02 W. The result of a frequency scan near the TM_{010} mode resonance is shown in Fig. 3. The linewidth was $\delta\nu = 32$ kHz at the resonance frequency of $\nu_p = 17994.7$ MHz. Near this resonance we observed other resonances of $TE_{11p=12}$ and TM_{011} modes at about 17.8 and 18.05 GHz, respectively. The overlap of the resonance signal tails with these neighboring resonances was negligible because of the very narrow linewidths. From (7) we found the loaded quality factor of $Q_L = 5.7 \times 10^5$. This value was obtained almost at the critical coupling condition as the reflected power was null at resonance, and therefore we estimated the unloaded quality factor of $Q_0 = 1 \times 10^6$. At 77 K, the quality factor was found to be $Q_L = 3 \times 10^3$, which was considerably lower than that of a bare copper cavity due to the lead–tin coating.

As for the time domain measurement, there are four transient signals to be observed: the build-up and the decay of the standing wave in the cavity measured through either transmission or reflection antenna. We applied microwave pulses with the power of $P_{in} = 5$ W. The transient signals for the decay of the standing wave for the TM_{010} mode are shown in Fig. 4. The pulse duration was 1, 10, and 100 ms. The decay constant, τ , which is defined as $W(t) \propto \exp(-t/\tau)$, was obtained from Fig. 4 to be 4.5 μ s (1 ms pulse), 3.9 μ s (10 ms), and 3.1 μ s (100 ms) for the reflection signal, and 4.6 μ s (1 ms), 4.2 μ s (10 ms), and 3.5 μ s (100 ms) for the transmission signals. From (8) we obtained the loaded quality factors of $Q_L = 2\pi\nu_p\tau = 4\text{--}5 \times 10^5$, which is almost consistent with the value obtained by the frequency domain measurement ($Q_L = 5.7 \times 10^5$). Note that even for $P_{in} = 5$ W input and 100 ms pulse duration, the quality

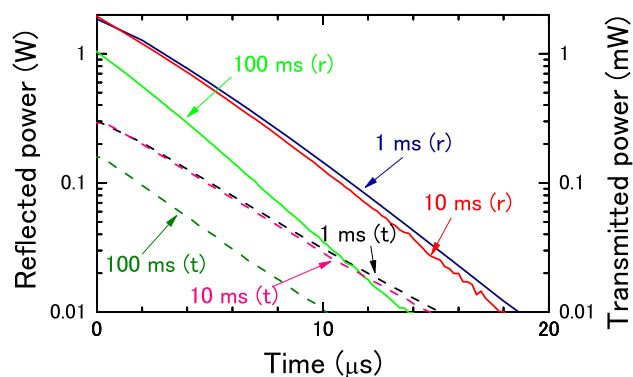


Fig. 4 Decay of the reflection and transmission signals for the pulses of 1, 10, and 100 ms. The time zero is at the end of each microwave pulse. The reflection signals are shown as solid lines with a label (r), and the transmission signals are shown as dashed lines with a label (t). Due to the drift of the resonance frequency during the 100 ms pulse, the stored energy at 0 μ s for the 100 ms pulse was slightly less than that for the 1 and 10 ms pulses

factor maintained almost the same value. We also tested the cavity with applying 5 W microwave and passing a pulsed beam of CH_3CN with a nitrogen carrier gas through the cavity. The CH_3CN beam passing the cavity was detected with a residual gas analyzer. We did not see decrease of the quality factor even after applying 10^4 beam pulses. We also did not see any discharge due to the intense microwave field.

4 Discussion

4.1 Quality factor

In Sect. 2, we have divided the microwave power loss of the cavity into three factors: the ohmic loss P_r , the diffraction loss P_d , and others P_{other} . Here, we estimate the values of P_r and P_d by the equations in section 2. As discussed in Sect. 2, the surface resistance of pure lead is estimated to be $R_s \simeq 23 \mu\Omega$ at 2.7 K and at 18 GHz. If we assume that the surface resistance of the lead-tin coating is the same as that of the pure lead, and also the residual surface resistance R_{res} is negligibly small, the corresponding quality factor becomes $Q_r = 2 \times 10^7$ for both the $TE_{11p} = 13$ and TM_{010} modes. On the other hand, the diffraction loss due to the end holes is negligibly small ($Q_d > 10^{10}$). Therefore, the maximum quality factor of the cavity we would expect is $Q_0 = 2 \times 10^7$ at 2.7 K.

The observed value of the unloaded quality factor, $Q_0^{obs} = 10^6$, for the TM_{010} mode is about one order of magnitude smaller than the predicted value of $Q_0 \simeq 2 \times 10^7$. The difference between the observed and predicted quality factors may be attributed to a larger residual surface resistance, R_{res} , than we estimated due to

imperfect lead-tin plating. Another origin of the loss could be due to contact resistances among parts of the cavity and antennas. Both of these losses can be technically improved in the future.

In order to obtain a higher quality factor, the simplest method is to lower the temperature of the cavity. If the R_{BCS} term of (3) limits the quality factor, we expect an increase by a factor of about 40 by lowering the temperature to 1.5 K. It is also noted that a high quality factor would be obtained using niobium, which is also commonly used as superconducting cavity material and has a higher critical temperature ($T_c = 9.25$ K) than lead.

In the decay measurements, we have observed that the resonance frequency shifted towards lower frequency by about 20 kHz when a 100-ms microwave pulse with a power of 5 W was applied. As a result, the stored energy was less for the 100 ms pulse than that with shorter pulses. The shift of the resonant frequency may be attributed to the change of the cavity condition due to heating by the microwaves. The temperature of the cavity increased by 0.2 K after the 100 ms pulse. The thermal expansion of the cavity length or diameter are negligibly small since the thermal expansion coefficient of copper is $1 \times 10^{-9} \text{ K}^{-1}$ at 2.7 K [49]. One possible cause of the shift of the resonant frequency may be the expansion of the semi-rigid cable input antenna, resulting in the change of the position of the antenna relative to the cavity. In fact, it was observed that the resonance shifted towards lower frequency for the TM_{010} mode by pushing the loop antenna into the cavity manually. Another origin of the frequency shift may be the change in the London penetration depth of the lead-tin coating due to the heating of the inner surface [50].

For a 10 ms pulse, the shift was about 5 kHz, while the shift was negligibly small for a 1 ms pulse. The shift of the resonant frequency due to the thermal effect becomes significant only when pulse lengths are longer than 10 ms. For the application of the cavity to the microwave decelerator, the accumulated duration of the microwave pulse train during a deceleration sequence is expected to be about 10 ms as will be described in Sect. 4.3, and therefore the thermal effect will not be significant. However, the effect has to be taken into account for the trapping application, as it requires a much longer pulse. The shift of the frequency must be compensated by shifting the microwave frequency to follow the drift of the resonance frequency.

In Sects. 4.2 and 4.3, we discuss the efficiency of the focusing and deceleration of molecules. For this discussion, we consider longer cavities with larger holes: (a) $d = 0.3$ m for the focusing with the TM_{010} mode and (b) $d = 1.0$ m for the deceleration with the TE_{11p} mode, with the hole dimension of $a_h = 2.5$ mm and $d_h = 4.5$ mm. For these cavities, we expect the quality factor of $Q_0 \simeq 10^7$ for

cavity (a) and $Q_0 \simeq 4 \times 10^6$ for cavity (b), based on the estimation of Q_d and Q_r for these cavities at 2.7 K and at 18 GHz. In the following sections, we assume these quality factors.

4.2 Molecular focusing

Here, we consider the focusing of molecular beams in a HFS state with the TM_{010} mode. The TM_{010} mode is ideal for the focusing, since the TM_{010} standing wave does not have any node that causes non-adiabatic state changes among degenerate internal states at zero electric field [31]. We discuss the transfer matrix for the motion of a molecule with this mode. From (1) and an expansion of $J_0(x) \sim 1 - x^2/4 + O(x^4)$, the radial confinement potential is approximated to be harmonic for $h|v_{\text{eg}} - v| \ll |E_0\mu_{\text{eg}}|$. We consider the two-dimensional motion of a molecule with no azimuthal velocity. We write the axial velocity as v_z , and express the radial position and velocity at the entrance and the exit of the cavity as $\{\rho_{\text{in}}, v_{\rho_{\text{in}}}\}$ and $\{\rho_{\text{out}}, v_{\rho_{\text{out}}}\}$, respectively. They are connected by the transfer matrix as

$$\begin{pmatrix} \rho_{\text{out}} \\ v_{\rho_{\text{out}}} \end{pmatrix} = \begin{pmatrix} \cos \frac{\alpha d}{v_z} & \frac{1}{\alpha} \sin \frac{\alpha d}{v_z} \\ -\alpha \sin \frac{\alpha d}{v_z} & \cos \frac{\alpha d}{v_z} \end{pmatrix} \begin{pmatrix} \rho_{\text{in}} \\ v_{\rho_{\text{in}}} \end{pmatrix}, \quad (11)$$

where $\alpha = \sqrt{E_0\mu_{\text{eg}}x_{01}^2/4a^2m}$ with m being the mass of the molecule.

As an example, we consider the use of the cavity (a) in section 4.1 for the focusing of a supersonic molecular beam of acetonitrile in the ground rotational state. We assume the input power of $P_{\text{in}} = 1$ W (i.e. $P_{\text{in}}Q_0 = 1 \times 10^7$ W), whose maximum amplitude of the electric field is $E_0 = 14$ kV/cm at the central axis of the cavity. With such an electric field, the ac Stark shift is almost linear as seen in Fig. 1. The parameter α becomes $2.4 \times 10^3 \text{ s}^{-1}$ for acetonitrile whose transition dipole moment is $\mu_{\text{eg}} = 2.26$ debye. Under such a condition, a supersonic molecular beam of acetonitrile becomes parallel, when the beam is emitted from a nozzle located 7 cm from the entrance hole of the cavity and the longitudinal velocity of the beam is $v_z \simeq 550$ m/s, which corresponds to a beam seeded in argon.

4.3 Molecular deceleration

Here, we consider the deceleration of a molecular beam in a HFS state with the TE_{11p} mode. The maximum kinetic energy, W_{tot} , to be removed by the decelerator is the product of the number of antinodes of the standing wave and the maximum ac Stark shift. We consider the use of cavity (b) in Sect. 4.1 with $P_{\text{in}} = 5$ W ($P_{\text{in}}Q_0 = 2 \times 10^7$ W) and $\nu = 18.3$ GHz, in order to decelerate

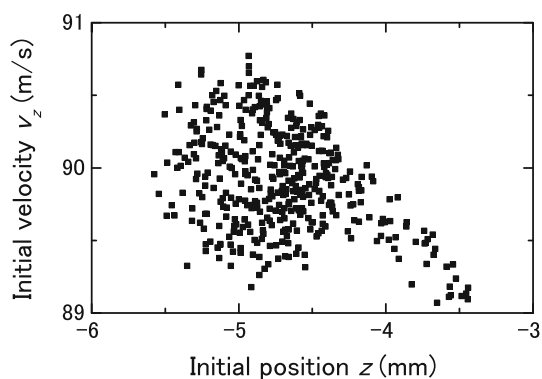


Fig. 5 Initial phase space plot of decelerated molecules obtained by the simulation. Each dot represents the position (z) and velocity (v_z) of a molecule at the nozzle position, which is successfully slowed down to $|v_z| < 5$ m/s by the microwave decelerator, where z is along the axis of the cavity. Molecules whose velocity is $|v_z| < 5$ m/s are eventually trapped in an antinode of the microwave standing wave inside the cavity. The $z=0$ point is taken at the inner surface of the entrance end cap

acetonitrile molecules. The resonance mode in the cavity is the $TE_{11p=80}$ mode. The maximum electric field is $E_0/2 = 11$ kV/cm, and $W_{\text{tot}}/k_B \simeq pE_0\mu_{\text{eg}}/4k_B = 25$ K for acetonitrile. In order to decelerate a molecular packet with a finite phase-space volume, there has to be a delay between the microwave switching time and the arrival of the synchronous molecule at the field maxima and minima [5]. By choosing an appropriate switching delay time, acetonitrile molecules with a kinetic energy of about 20 K will be completely stopped.

In order to decelerate molecules, the standing wave has to be switched on and off much faster than the flight time of a molecule per each potential well. The flight time is obtained from $\lambda_g/2v_z$ where $\lambda_g = [(v/c)^2 - (x'_{11}/2\pi a)^2]^{-1/2}$ is the guide wavelength. From the decay of the standing wave in the cavity given in (8), it is required that $Q_L \ll \pi v \lambda_g / v_z = 1.6 \times 10^7$ for acetonitrile with a kinetic energy of 20 K, corresponding to a translational velocity of 90 m/s. This requirement is satisfied in the present case where $Q_L \simeq Q_0/2 = 2 \times 10^6$.

Figure 5 shows a result of the Monte-Carlo simulation of the deceleration of acetonitrile in the ground rotational state with cavity (b). Acetonitrile molecules are assumed to be initially distributed randomly in a six-dimensional cube with a phase space of $|x|, |y| < 1.5$ mm, $-6 < z < -3$ mm, $|v_x|, |v_y| < 4$ m/s, and $89 < v_z < 91$ m/s. The x, y Cartesian coordinate axes lie perpendicular to the direction of the molecular beam (the z axis). The initial condition of the synchronous molecule is $x, y = 0$ mm, $z = -5$ mm, $v_x, v_y = 0$ m/s, and $v_z = 90$ m/s. The timing of the switching of the standing wave is determined such that the synchronous molecule loses its kinetic energy by 0.27 K at

each potential well. Trajectories of other molecules are calculated with these switching times. A packet of molecules whose initial phase-space distribution is shown in Fig. 5, which amounts to about 5% of the total molecules in the phase-space cube, is decelerated and eventually trapped in an antinode located at $z = 0.94$ m. The deceleration time from 90 m/s to $|v_z| < 5$ m/s is about 20 ms, and the accumulated duration of the microwave pulses is about 10 ms. As described in Sect. 3, we have observed that our superconducting cavity retains its quality factor of $Q_0 \simeq 10^6$ even for a 100 ms pulse of $P_{\text{in}} = 5$ W. Our cavity already satisfies the condition for efficient deceleration of acetonitrile molecules.

5 Conclusions

We have discussed the use of a superconducting cylindrical cavity for the control of translational motion of polar molecules. We have constructed a lead-tin plated copper cavity and examined its performance at 2.7 K and at 18 GHz. It is confirmed that the cavity can accept at least 5 W microwave power for 100 ms while keeping the high quality factor of $Q_0 \simeq 10^6$. The efficiency of the focusing and deceleration of molecular beams is quantitatively estimated for a cavity with practical cavity parameters. The *focusing* of HFS states becomes possible by using the TM_{010} mode. The TM_{010} mode is ideal for focusing because no nodes exist in the cavity and the field pattern provides an axially symmetric harmonic potential. This focusing method will be useful for various applications, as it provides highly collimated beams of polar molecules. One potential application lies in molecule-based precision measurements such as the measurement of the electron electric dipole moment [13]. The *deceleration* of molecules in HFS states can be performed using the TE_{11p} mode. The energy removal of the deceleration is about 20 K for 5 W microwave power for a molecule with a permanent dipole moment of about 4 debye. The main limitation of this deceleration method is the switching speed of the standing wave in a high-quality-factor cavity, but a combination with an appropriate precooling method such as buffer-gas cooling can overcome this issue. An advantage of the present method is that the radial confinement of this microwave decelerator is static, which is more stable than the dynamic confinement of the alternate gradient focusing decelerator [16]. The microwave decelerator will establish the radial confinement and axial deceleration simultaneously as in the case of the Stark decelerator for LFS states. The microwave deceleration technique is suited to the deceleration of pre-cooled molecules in HFS states down to zero velocity.

Acknowledgments We acknowledge D. DeMille and G. Meijer for their helpful advice and M. Schnell, A. Simon, H. Odashima, M. Kajita, F. Matsushima, and K. Kobayashi for their fruitful discussion. We also thank B. Ramshaw and D. Bonn for helping us perform the electroplating. This work is supported by an NSERC Discovery Grant and funds from CFI to CRUCS at UBC. This work is also partially supported by Grant-in-Aid for Scientific Research of JSPS (19840021, 21740300, 22104504), Matsuo foundation, Inamori foundation. K.E. acknowledges support from the Excellent Young Researchers Overseas Visit Program of JSPS for allowing him to visit UBC to perform this research.

References

- J. Reuss, in *Atomic and Molecular Beam Methods*, ed. by G. Scoles, D. Bassi, U. Buck, D. Lainé (Oxford University Press, New York, 1988)
- O. Stern, *Z. Phys.* **7**, 249 (1921)
- W. Gerlach, O. Stern, *Z. Phys.* **9**, 353 (1922)
- J.D. Weinstein et al., *Nature (London)* **395**, 148 (1998)
- H.L. Bethlem et al., *Nature* **406**, 491 (2000)
- J. van Veldhoven, H.L. Bethlem, G. Meijer, *Phys. Rev. Lett.* **94**, 083001 (2005)
- S.A. Rangwala, T. Junglen, T. Rieger, P.W.H. Pinkse, G. Rempe, *Phys. Rev. A* **67**, 043406 (2003)
- H. Tsuji, T. Sekiguchi, T. Mori, T. Momose, H. Kanamori, *J. Phys. B At. Mol. Opt. Phys.* **43**, 095202 (2010)
- N. Vanhaecke, U. Meier, M. Andrist, B.H. Meier, F. Merkt, *Phys. Rev. A* **75**, 031402 (2007)
- E. Narevicius et al., *Phys. Rev. A* **77**, 051401 (2008)
- L.D. Carr, D. DeMille, R.V. Krems, J. Ye, *New J. Phys.* **11**, 055049 (2009)
- R.V. Krems, W.C. Stwalley, B. Friedrich (eds.), *Cold Molecules, Theory, Experiment, Applications* (CRC Press, Boca Raton, 2009)
- J.J. Hudson et al., *Nature* **473**, 493 (2011)
- T. Junglen, T. Rieger, S.A. Rangwala, P.W.H. Pinkse, G. Rempe, *Phys. Rev. Lett.* **92**, 223001 (2004)
- T.E. Wall et al., *Phys. Rev. A* **80**, 043407 (2009)
- H.L. Bethlem, A.J.A. van Roij, R.T. Jongma, G. Meijer, *Phys. Rev. Lett.* **88**, 133003 (2002)
- M.R. Tarbutt et al., *Phys. Rev. Lett.* **92**, 173002 (2004)
- K. Wohlfart et al., *Phys. Rev. A* **77**, 031404 (2008)
- H.J. Loesch, B. Scheel, *Phys. Rev. Lett.* **85**, 2709 (2000)
- M. Strebel, S. Spieler, F. Stienkemeier, M. Mudrich, *Phys. Rev. A* **84**, 053430 (2011)
- R. Fulton, A.I. Bishop, P.F. Barker, *Phys. Rev. Lett.* **93**, 243004 (2004)
- R. Fulton, A.I. Bishop, M.N. Shneider, P.F. Barker, *Nat. Phys.* **2**, 465 (2006)
- Z. Lan, Y. Zhao, P.F. Barker, W. Lu, *Phys. Rev. A* **81**, 013419 (2010)
- V. Vuletić, S. Chu, *Phys. Rev. Lett.* **84**, 3787 (2000)
- S. Kuma, T. Momose, *New. J. Phys.* **11**, 055023 (2009)
- Z. Lan, Y. Zhao, P.F. Barker, W. Lu, *Phys. Rev. A* **81**, 013419 (2010)
- D. DeMille, D.R. Glenn, J. Petricka, *Eur. Phys. J. D* **31**, 375 (2004)
- D.R. Glenn, Ph.D. thesis, Yale University (2009)
- K. Enomoto, T. Momose, *Phys. Rev. A* **72**, 061403 (2005)
- R. Hill, T. Gallagher, *Phys. Rev. A* **12**, 451 (1975)
- H. Odashima, S. Merz, K. Enomoto, M. Schnell, G. Meijer, *Phys. Rev. Lett.* **104**, 253001 (2010)
- S. Merz, N. Vanhaecke, W. Jäger, M. Schnell, G. Meijer, *Phys. Rev. A* **85**, 063411 (2012)
- M. Kajita, A.V. Avdeenkov, *Eur. Phys. J. D* **41**, 499 (2007)
- S.V. Alyabyshev, R.V. Krems, *Phys. Rev. A* **80**, 033419 (2009)
- S.E. Maxwell et al., *Phys. Rev. Lett.* **95**, 173201 (2005)
- P. Schmäser, *Prog. Part. Nucl. Phys.* **49**, 155 (2002); and references therein.
- J.M. Raimond, M. Brune, S. Haroche, *Rev. Mod. Phys.* **73**, 565 (2001)
- H. Walther, B.T.H. Varcoe, B.-G. Englert, T. Becker, *Rep. Prog. Phys.* **69**, 1325 (2006)
- J. Gadhi, A. Lahrouni, J. Legrand, J. Demaison, *J. Chim. Phys.* **92**, 1984 (1995)
- C.G. Montgomery, *Technique of Microwave Measurements* (McGraw-Hill, New York, 1947)
- D.M. Pozar, *Microwave Engineering* (Wiley, Hoboken, 2005)
- J. Halbritter, *Z. Phys.* **238**, 466 (1970)
- H.A. Bethe, *Phys. Rev.* **66**, 163 (1944)
- C.J. Bouwkamp, *Rep. Prog. Phys.* **17**, 35 (1954)
- N.A. McDonald, *IEEE Trans. Microwav Theory Tech.* **20**, 689 (1972)
- A. Roberts, *J. Opt. Soc. Am. A* **4**, 1970 (1987)
- A.Y. Nikitin, D. Zueco, F.J. García-Vidal, L. Martín-Moreno, *Phys. Rev. B* **78**, 165429 (2008)
- W.H. Warren Jr, W.G. Bader, *Rev. Sci. Instrum.* **40**, 180 (1968)
- D.A. Ackerman, A.C. Anderson, *Rev. Sci. Instrum.* **53**, 1657 (1982)
- W.N. Hardy, D.A. Bonn, D.C. Morgan, R. Liang, K. Zhang, *Phys. Rev. Lett.* **70**, 3999 (1993)